A di-iron(III) mu-oxido complex as catalyst precursor in the oxidation of alkanes and alkenes

Das, Biswanath

2022-06

Das , B , Al-Hunaiti , A , Carey , A , Lidin , S , Demeshko , S , Repo , T & Nordlander , E 2022 , ' A di-iron(III) mu-oxido complex as catalyst precursor in the oxidation of alkanes and alkenes ' , Journal of Inorganic Biochemistry , vol. 231 , 111769 . https://doi.org/10.1016/j.jinorgbio.2022.111769

http://hdl.handle.net/10138/343960
https://doi.org/10.1016/j.jinorgbio.2022.111769

Journal of Inorganic Biochemistry 231 (2022) 111769

Contents lists available at ScienceDirect

Journal of Inorganic Biochemistry

journal homepage: www.elsevier.com/locate/jinorgbio

A di-iron(III) μ-oxido complex as catalyst precursor in the oxidation of alkanes and alkenes☆

Biswanath Das [a,1], Afnan Al-Hunaiti [b,2], Akina Carey [b], Sven Lidin [c], Serhiy Demeshko [d], Timo Repo [b,*], Ebbe Nordlander [a,*]

[a] Chemical Physics, Department of Chemistry, Lund University, Box 124, SE-221 00 Lund, Sweden
[b] Department of Chemistry, Laboratory of Inorganic Chemistry, University of Helsinki, 00014 Helsinki, Finland
[c] Center for Analysis and Synthesis, Department of Chemistry, Lund University, Box 124, SE-221 00 Lund, Sweden
[d] Institute for Inorganic Chemistry, Georg-August-University Göttingen, Tammanstrasse 4, D-37077 Göttingen, Germany

ARTICLE INFO

Keywords:
Catalysis
Hydroxylation
Epoxidation
Peroxide complex
Metal-oxido complex
Iron

ABSTRACT

The oxido-bridged diiron(III) complex $[Fe_2(\mu\text{-}O)(\mu\text{-}OAc)(DPEAMP)_2](OCH_3)$ (**1**), based on a new unsymmetrical ligand with an N_4O donor set, *viz*. [2-((bis(pyridin-2-ylmethyl)amino)methyl)-6-((ethylamino)methyl)-4-methylphenol (HDPEAMP)], has been prepared and characterized by spectroscopic methods and X-ray crystallography. The crystal structure of the complex reveals that each Fe(III) ion is coordinated by three nitrogen and three oxygen donors, two of which are the bridging oxido and acetate ligands. Employing H_2O_2 as a terminal oxidant, **1** is capable of oxidizing a number of alkanes and alkenes with high activity. The catalytic oxidation of 1,2-dimethylcyclohexane results in excellent retention of configuration. Monitoring of the reaction of **1** with H_2O_2 and acetic acid in the absence of substrate, using low-temperature UV–Vis spectroscopy, suggests the *in situ* formation of a transient $Fe(III)_2$-peroxido species. While the selectivity and nature of oxidation products implicate a high-valent iron-oxido complex as a key intermediate, the low alcohol/ketone ratios suggest a simultaneous radical-based process.

1. Introduction

Oxidations of hydrocarbons are mainstay reactions in the chemical industry that are used, *inter alia*, for the production of alcohols, ketones, carboxylic acids, and peroxides. Therefore, there is a great impetus to continuously improve such reactions, and develop new methods for catalytic C-H bond oxidation. The high thermodynamic stability of alkane C-H bonds makes efficient activation of such bonds a challenging task. Despite having higher C-H bond dissociation energies, some alkenes and aromatic compounds show considerably higher reactivity towards oxidation than alkanes due to the presence of π electrons [1], and selective oxidations of complex organic substrates are therefore difficult.

In nature, the most inert alkane, methane (for which the C-H bond dissociation energy is 104 kcal mol^{-1}), is oxidized to methanol by the methane monooxygenase enzymes [2], *viz*. soluble methane monooxygenase (sMMO) [3] and particulate methane monooxygenase (pMMO) [4]. Structures of both proteins have been determined by X-ray

Abbreviations: HDPEAMP, [2-((bis(pyridin-2-ylmethyl)amino)methyl)-6-((ethylamino)methyl)-4-methylphenol; PTEBIA, (2-((2,4-dimethylphenyl)thio)-N,N-bis((1-methyl-benzimidazol-2-yl)methyl)ethanamine; DPCPMPP, 3-[(3-{[bis(pyridin-2-ylmethyl)amino]methyl}-2-hydroxy-5-methylbenzyl)(pyridin-2-ylmethyl)amino]propanoate; H_2IPCPMP, 2-{*N*-isopropyl-*N*-[(2-pyridyl)methyl]aminomethyl}-6-{*N*(carboxymethyl)-*N*-[(2-pyridyl)methyl] aminomethyl}-4-methylphenol; BBP, 2,6-bis(1-methyl-1H-benzo[*d*]imidazol-2-yl)pyridine; pca-, pyrazine-2-carboxylate; sMMO, soluble methane monooxygenase; pMMO, particulate methane monooxygenase; Piv, pivalate; TBHP, tert-butyl hydroperoxide; OBz, benzoate; BDEs, bond dissociation energies; MeCN, Acetonitrile; OAc, Acetate; BPCINOL, (N-(2-hydroxybenzyl)-N-(2-pyridylmethyl)[(3-chloro)(2-hydroxy)]propylamine); TPA, tri(picolyl)amine; *m*-CPBA, *meta*-chloroperoxybenzoic acid; A/K ratio, alcohol to ketone ratio.

☆ Richard H. Holm *in memoriam*

* Corresponding authors.
E-mail addresses: Timo.Repo@helsinki.fi (T. Repo), Ebbe.Nordlander@chemphys.lu.se (E. Nordlander).
[1] Present address: Department of Organic Chemistry, Section for Chemistry, Stockholm University, Svante Arrhenius Väg 16C, SE-106 91 Stockholm, Sweden.
[2] Present address: Chemistry Department, School of Science, University of Jordan, Amman 11942, Jordan.

https://doi.org/10.1016/j.jinorgbio.2022.111769
Received 5 December 2021; Received in revised form 10 February 2022; Accepted 10 February 2022
Available online 17 February 2022

crystallography [2,3b,5]. In sMMO, a carboxylate-bridged dinuclear iron center (Fig. 1) is the active site that performs the oxidation reaction [2,3]. Even though the structure of pMMO is known, the location and mechanism of the active site in this enzyme is still not completely understood, but it is believed that a copper cluster is the reactive center that hydroxylates methane [4].

Being relatively stable and easier to isolate than the membrane-bound protein pMMO, sMMO has been the subject of intense research [3]. Although significant advances have been made in understanding the reaction mechanism and the nature of the intermediates formed in sMMO-catalyzed reactions, several key steps remain subject to debate [3d]. The instability of higher oxidation states of iron, which are implicated in the active catalytic intermediate of sMMO, makes it very difficult to isolate and identify the reactive intermediate(s) [3d,6]. Nevertheless, it is clear that the reduced, diferrous, form of the active site binds and activates dioxygen to form a Fe(III)(μ-peroxido)Fe(III) intermediate ("intermediate P"). The structure of this intermediate has not been unambiguously determined, but it is known that both oxygens are symmetrically coordinated to the Fe(III) centers [3d,e,6,7]. Intermediate P spontaneously converts to intermediate Q, which is proposed to contain an antiferromagnetically coupled high spin dioxido-bridged Fe(IV)(μ-oxido)$_2$Fe(IV) diamond core [3d,e,6] and is thought to be the active catalyst. Valence tautomers of this intermediate, *e.g.* an O=Fe(V)(μ-oxo)(Fe(III) core, have been proposed to be (alternative) active forms of the oxidant [3e,8].

Several bio-inspired iron catalysts that are effective in the selective oxidation of relatively complicated organic substrates have been developed. In a series of investigations, White and coworkers have been able to successfully predict the selectivity of aliphatic C-H bond oxidation by mononuclear iron catalysts on the basis of the presence of carboxylate-containing directing groups as well as electronic and steric properties around the C-H bonds [9]. Using a series of mononuclear iron (II) – bis(trifluoromethanesulfonate) complexes, Britovsek and coworkers have been able to establish a correlation between the strength of the ligand field and the stability of the complexes with the activity and the selectivity with respect to the catalytic oxidation of cyclohexane [10]. They also demonstrated the possibility of changing the reaction pathway from a metal-based mechanism (more selective products) to Fenton-type chemistry by changing the ligand environment, *e.g.* for [Fe(TPA)(OTf)$_2$] (TPA = tri(picolyl)amine; OTf = trifluoromethanesulfonate); the alkane oxidation proceeds *via* a metal-based mechanism while the corresponding complex of *N,N*-bis((dimethylamino)methyl)-*N,N*-dimethylmethanediamine favors Fenton-type chemistry [11].

Several dinuclear oxido-bridged diiron complexes have also been explored as potential oxidation catalysts and model complexes for the active site of sMMO [6]. This includes model complexes containing Fe(IV)(μ-oxido)$_2$Fe(IV) diamond cores that emulate intermediate Q, which have recently been published [12].We have previously studied the oxido- and carboxylato-bridged dinuclear complex [{Fe(HIPCPMP)}$_2$(μ-O)(μ-Piv)]$^+$ ((Piv = pivalate, IPCPMP = 2-[N-isopropyl-N-{(2-pyridyl)methyl}-aminomethyl] - 6 - [N - (carboxylmethyl) -N - {(2-pyridyl)methyl}-aminomethyl]-4-methylphenol), Fig. 2) [13a]. This complex was found to catalyze the oxidation of alkanes by H_2O_2 to form corresponding alcohols and ketones. The alcohol/ketone ratios and stereospecificity of alkane hydroxylation indicated that both metal-based and free radical oxidation mechanisms were occurring [13a]. Similar observations were made in C-H activation studies using two different μ-oxido complexes, [Fe$_2$(μ-O)(LiDPCPMPP)$_2$](ClO$_4$)$_2$ [13b] and [Fe$_2$(μ-O)Cl$_2$(PTEBIA)$_2$] (CF$_3$SO$_3$)$_2$, as catalysts/catalyst precursors [13c] (Fig. 2, LiDPCPMPP = lithium 3-[(3-{[bis(pyridin-2-ylmethyl)amino]methyl}-2-hydroxy-5-methylbenzyl)(pyridin-2-ylmethyl)amino]propanoate; PTEBIA = (2-((2,4-dimethylphenyl)thio)-N,N-bis ((1-methyl-benzimidazol-2-yl)methyl)ethanamine). These complexes were found to catalyze the oxidation of alkanes and alkenes by H_2O_2/CH_3COOH to form corresponding alcohols and ketones by partial metal-based oxidation, in tandem with free-radical oxidation [13].

Here we present the synthesis of the new unsymmetric pro-ligand 2-((bis(pyridin-2-ylmethyl)amino)methyl)-6-((ethylamino)methyl)-4-methylphenol (HDPEAMP), and preparation of the μ-oxido diiron(III) complex [Fe$_2$(μ-O)(μ-OAc)(DPEAMP)$_2$](OCH$_3$) (**1**) (OAc = acetate), which has been characterized by Mössbauer spectroscopy, cyclic voltammetry, IR and UV–Vis spectroscopies, as well as X-ray crystallography. The ability of the new diiron complex to function as a (pre) catalyst for the oxidation of a number of alkanes and alkenes, using H_2O_2 and CH_3COOH (1:1) as terminal oxidant(s), has been investigated.

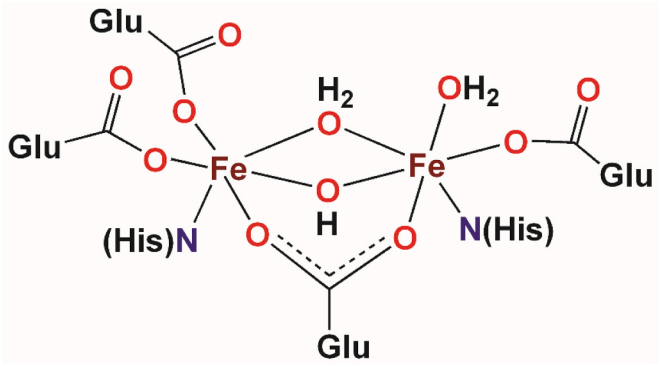

Fig. 1. Schematic depiction of the oxidized diferric form of the active site in the hydroxylase subunit of soluble methane monooxygenase (MMOHox) [3].

2. Results and discussion

2.1. Synthesis and characterization of ligand and complex

The new pro-ligand HDPEAMP [2-((bis(pyridin-2-ylmethyl)amino)methyl)-6-((ethylamino)methyl)-4-methylphenol], with a potential N$_4$O donor set, was synthesized from 2-hydroxy-3-(hydroxymethyl)-5-methylbenzaldehyde (**a**) in an overall yield of 51% (Scheme 1). Condensation of dipicolyl amine (bis(pyridin-2-ylmethyl)amine) with **a**, followed by reduction with NaBH(OAc)$_3$, led to 2-((bis(pyridin-2-ylmethyl)amino)methyl)-6-(hydroxymethyl)-4-methylphenol (**b**). The latter product was reacted with an excess of thionyl chloride to convert the primary alcohol moiety to a chloride, yielding (**c**). The chloride substituent was replaced by a primary amine (ethyl amine in this case) by reflux for three hours, in the presence of a catalytic amount of triethyl amine, to form HDPEAMP. (See Scheme 1)

Addition of one equivalent of iron(II) acetate to a methanolic solution of HDPEAMP, followed by addition of one equivalent of NaClO$_4$, led to the formation of complex **1** (Scheme 2). An immediate color change (from pale yellow to dark green and then to dark brown) of the ligand solution on addition of the iron salt indicated complexation, and this was verified by IR and UV–Vis spectroscopy, as well as X-ray crystallography.

An acetonitrile solution (0.2 mM) of **1** exhibits three absorption maxima at around 498 nm, 334 nm and 289 nm. The absorption maximum at 498 nm is assigned to the phenolate to a Fe(III) pπ to dπ* ligand-to-metal charge transfer (LMCT) absorption [14]. The absorption maximum at 334 nm is in the so called öxo dimer region and is characteristic of the Fe-O-Fe moiety, as has been observed for similar (μ-oxido)diiron(III) complexes [14–16]. The spectroscopic and magnetic properties of Fe(III)-O-Fe(III) complexes are influenced by the angle of that unit [17]. As **1** is a di-bridged complex with an Fe-O-Fe angle of approximately 128^o (*cf.* crystallographic results, below), thus lying in the interval 114 < **128** < 130^o [14], the absorption maximum at 289 nm can be attributed to an overlap of π derived transitions from the bridging O^{oxido} to the Fe(III) ions, as has been discussed by several authors [14–16]. A blue shift of the UV/Vis spectrum occurred on changing the

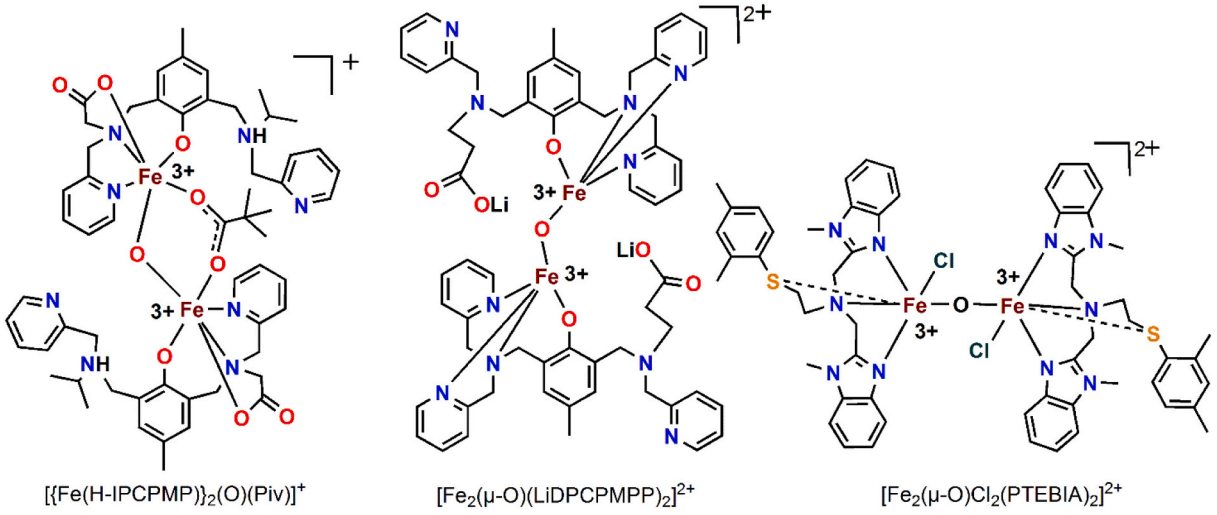

Fig. 2. Schematic depiction of Fe(III)-O-Fe(III) complexes based on the the ligands HIPCPMP, DPCPMPP and PTEBIA (see text) [13].

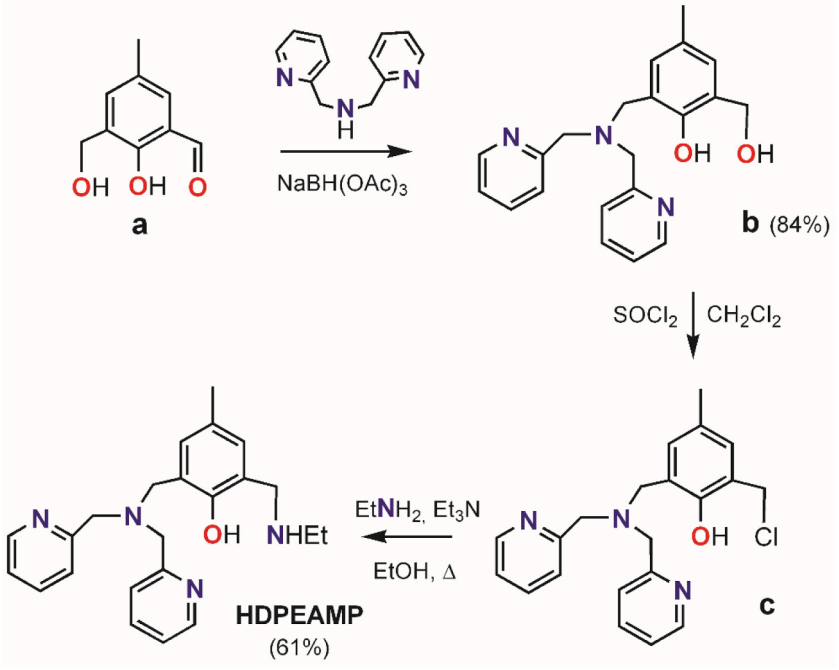

Scheme 1. A schematic presentation of the synthesis of HDPEAMP.

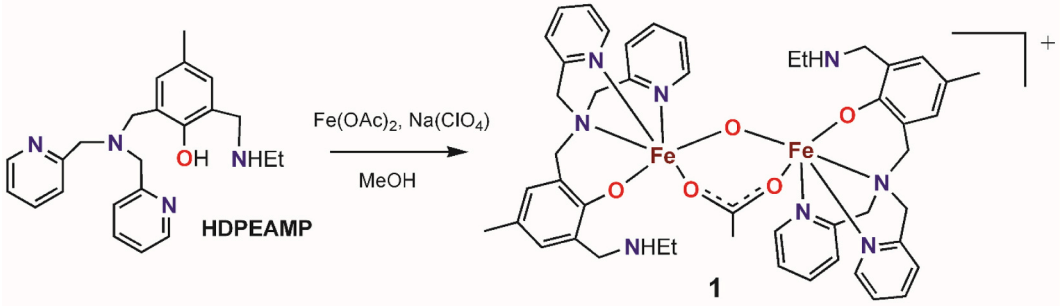

Scheme 2. Schematic depiction of the synthesis of complex **1**.

pH from 5 to 10 by titration with triethylamine. A clear isosbestic point was found at 487 nm (Fig. S2), which corroborates the presence of a single species during pH titration. Interestingly, addition of 20 μl of acetic acid to the acetonitrile solution led to a prominent red shift (by 40 nm) of the 498 nm band, indicating stronger charge transfer from the phenoxide moiety to Fe(III) (Fig. 5a, *vide infra*). This phenomenon is most likely due to protonation of the bridging oxido ion, resulting in a weaker Fe-OH (O^{oxido}) bond.

The IR spectrum of **1** shows characteristic resonances for a bridging carboxylate and an Fe-O-Fe moiety [14–16]. The difference between asymmetric and symmetric stretching frequencies ($\Delta\nu = \nu_{asym}$- ν_{sym}) of carboxylate moieties in IR spectra has been used extensively to understand the ligation mode of carboxylates [18]. An empirical correlation indicates that the $\Delta\nu$ value is related to unidentate coordination of a carboxylate moiety when $\Delta\nu > 200\ cm^{-1}$ or bridging when it is $100 < \Delta\nu < 200\ cm^{-1}$. The separation between the two sharp peaks at 1605 and 1478 ($\Delta\nu = 127\ cm^{-1} < 200\ cm^{-1}$) suggests a bridging mode of the carboxylate moiety and the sharp resonances at 849 cm^{-1} and 559 cm^{-1} in the IR spectra can be assigned to asymmetric and symmetric Fe-O stretching frequencies of the Fe-O-Fe unit, respectively [14].

The zero-field ^{57}Fe Mössbauer spectrum of the crude dark brown powder of $[Fe_2O(OAc)(DPEAMP)_2](OCH_3)$ (Fig. S2) could be fitted to one doublet with $\delta = 0.49$ mm/s, and $\Delta E_Q = 1.38$ mm/s, consistent with the presence of high spin Fe(III) and in close agreement with observed Mössbauer spectra for similar Fe(III)-O-Fe(III) complexes [19].

2.2. Crystal and molecular structure of $[Fe_2O(OAc)(DPEAMP)_2](OCH_3)$ (1)

In order to ascertain the molecular structure of **1**, its crystal structure was determined. The molecular structure of the cationic diiron complex is shown in Fig. 3. Crystallographic data are collated in Table S1 (Supplementary Material). The crystal structure reveals that complex **1** is a μ-oxido diiron(III) complex with two equivalents of the unsymmetrical ligand in each molecule (Fig. 3).

The Fe(III) centers are in N_3O_3 coordination environments with distorted octahedral geometries. Although disorder and the lack of identification of all solvent molecules led to a relatively high R factor (R1 ($I \geq 2\sigma$) = 0.086, cf. Table S1 and the Experimental Section), the core structure of the complex (Fig. 3) is well resolved and permits discussion of interatomic distances and bond angles. The two iron ions are 3.223(1) Å apart from each other, resembling that of 3.1 Å in the active site of MMOH from *Pseudomonas stutzeri* OX1 [20]. The Fe-O-Fe moiety creates an angle of 127.62(2)°, which is very similar to that found in the related $[\{Fe(H\text{-}IPCPMP)\}_2(\mu\text{-}O)(Piv)]^+$ complex [13a]. Similar Fe-Fe distances and Fe-O-Fe angles have been observed by Norman and coworkers for a number of μ-oxido diiron(III) monocarboxylate complexes where the two Fe(III) ions were separated by 3.09–3.11 Å and the Fe-O-Fe angles ranged from 115° to 125° [15]. In addition to the bridging oxido moiety, the two Fe(III) ions are also bridged by the acetate, with O^{ac}-$C1^{ac}$-O^{ac_i} and O^{oxido}-Fe-O^{ac} angles of 131.76(4)° and 101.62(2)°, respectively, with equal Fe1-O^{ac} and $Fe1^{i}$-O^{ac_i} distances of 1.98(0) Å. (Fig. 3).

A terminal phenoxide moiety from the DPEAMP ligand is coordinated to each Fe(III) center in **1**, with a Fe-O3(phenoxide) bond distance of 1.952(1) Å. It has been shown that phenoxide moieties ligated to Fe (III) may stabilize higher oxidation states (IV or even V) of iron [21] or might act as non-innocent ligands to form coordinated phenoxyl radical moieties [22,23]. There is also a non-coordinated NHEt moiety with the amine nitrogen being quite well separated (by 5.68(2) Å) from the Fe (III) center(s). This pendant amine moiety is well positioned for secondary non-covalent interactions with the metal centers and/or substrates in solution and may be considered to function as a partial model for the second coordination sphere found in metallobiosites [13c,24]. In this respect, it is reminiscent of the "dangling" tertiary amine group of the ligand IPCPMP in $[\{Fe(H\text{-}IPCPMP)\}_2(\mu\text{-}O)(\mu\text{-}Piv)]^+$ (*cf.* Fig. 2). Due to the flexibility of the terminal C-N-C-C moiety, the non-coordinated secondary amine is disordered but this moiety becomes ordered once it is coordinated to a metal ion, as evidenced by the crystal structure of $[Fe_2Mn(DPEAMP)_2]$ $(ClO_4)_2$ [25]. The methoxide ion functions as a counter-ion without any direct interaction with the complex, as has been found in some previously reported systems [26,27].

2.3. Electrochemical studies

The cyclic voltammogram of **1** in acetonitrile solution (1 mM) shows four irreversible redox couples (Fig. S3). The irreversible peaks at −0.56 V and − 1.05 V can be attributed to the Fe(III)Fe(*III*)/Fe(III)Fe(*II*), and Fe(*III*)Fe(II)/Fe(*II*)Fe(II) couples, respectively. A similar kind of redox behavior has been observed by Neves and coworkers for $[Fe(III)_2(BPCINOL)_2(H_2O)_2]^{2+}$ (BPCINOL = (N-(2-hydroxybenzyl)-N-(2-pyridylmethyl)[(3-chloro)(2-hydroxy)]propylamine)] [28]. The other

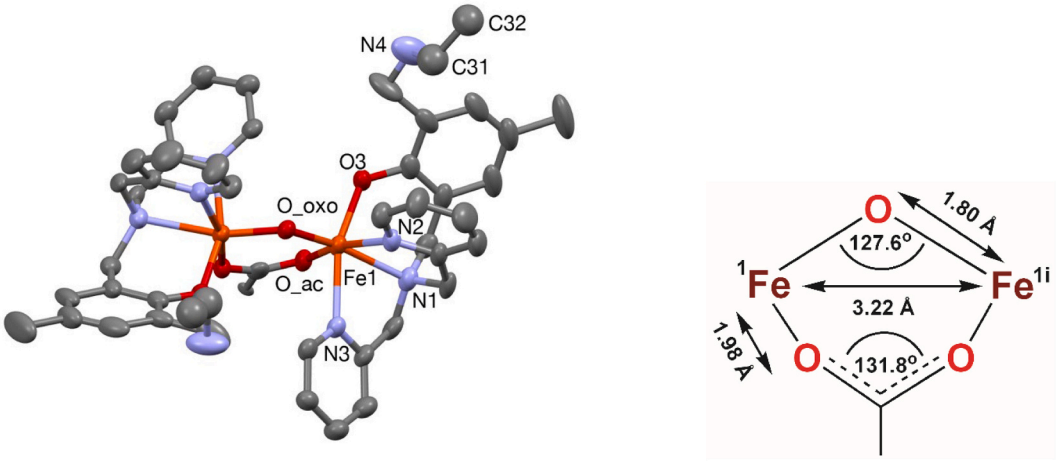

Fig. 3. (a) A Mercury representation of the molecular structure of $[Fe_2O(OAc)(DPEAMP)_2]^+$. Thermal ellipsoids are plotted at 30% probability; all hydrogen atoms have been omitted for the sake of clarity. The ethyl moiety C31-C32 has been plotted as (isotropic) spheres due to their large thermal parameters (see the Experimental Section for discussion of disorder in the crystal). (b) Core angles and distances in the $Fe_2O(OAc)$ unit. Selected bond distances (Å) and angles (deg): Fe1-$Fe1^{i}$ 3.223(1)[b], Fe1-O^{ac} 1.980 (0), Fe1-O^{oxo} 1.796(1), Fe1-O3 1.952(1), Fe1-N1 2.277(3), Fe1-N2 2.153(1), Fe1-N3 2.219(3), Fe1-O-$Fe1^{i}$ 127.61(2), O^{ac} –$C1^{ac}$- O^{ac_i} 131.76 (4), N2-Fe1-N1 76.58(5), N1-Fe1-N3 72.29(5), N2-Fe1-O3 86.70(3), N3-Fe1-O^{ac} 86.35(5), N3-Fe1-O^{oxo} 93.55(1), N1-Fe1-O^{oxo} 165.06(2), N3-Fe1-O^{oxo} 93.31(1), O3-Fe1-O^{ac} 94.59(2), O3-Fe1-O^{oxo} 102.89(4).

irreversible peaks at 0.72 V and 1.22 V may be attributed to the Fe(II)Fe(*II*)/Fe(II)Fe(*III*) and Fe(*II*)Fe(III)/Fe(*III*)Fe(III) couples, respectively. The irreversibility appears to be due to chemical irreversibility caused by changes in the coordination environment of the iron ion upon reduction [28].

2.4. Reactivity studies

Several oxido and/or carboxylate-bridged diiron complexes have been studied as alkane oxidation catalysts with the purpose of establishing structural and functional models for Fe-dependent oxygenases [29]. Using *tert*-butyl hydroperoxide (TBHP) as oxidant and the dinuclear complex $[Fe(III)_2(\mu\text{-}O)(NO_2)_2(BBP)_2(CH_3OH)_2](NO_3)_2$ [BBP = 2,6-bis(1-methyl-1H-benzo[*d*]imidazol-2-yl)pyridine] as a catalyst, Wang *et al.* [30] found 51% substrate conversion in the oxidation of cyclohexane with an alcohol/ketone (A/K) ratio of 1.2, indicating the involvement of freely diffusing carbon-centered radicals. On the other hand, Itoh et al. reported that the oxidation of cyclohexane by *meta*-chloroperoxybenzoic acid (*m*-CPBA), using the dinuclear $[Fe^{III}_2(\mu\text{-}O)((S)\text{-}L)(OBz)_2](ClO_4)$ [(*S*)-LH_2 = (*S*)-3,3-bis[*N*,*N*-bis(2-pyridylmethyl)aminomethyl]-1,1-bi-2-naphthol; OBz = benzoate] complex as catalyst, gave high A/K ratios and high normalized 3°/2 °C-H selectivity values for adamantane oxidation, indicating a metal-based mechanism [29]. However, when H_2O_2 or TBHP was used as oxidants instead of *m*-CPBA, radical-based mechanisms were favored [31], clearly demonstrating that the nature of the mechanism is dependent on the nature of the oxidant/oxo atom donor.

In the present study, several combinations of solvents and oxidants have been investigated (Table 1). The ability of **1** to catalyze the oxidation of alkanes was studied in MeCN at 40 °C, using H_2O_2 as an oxidant and cyclohexane as a model substrate (Table 2). Although *m*-CPBA is also commonly used as a terminal oxidant [32], H_2O_2 is preferable as H_2O is the only sideproduct from the oxidant. High reactivity with low alcohol to ketone (A/K) ratio is characteristic for **1** when acetic acid is used as an additive (Table 2, entry 2). Carboxylic acids are commonly added when hydrogen peroxide is used as an oxidant, especially in the case of olefin expoxidation [33]. A carboxylic acid additive assists the heterolytic cleavage of the O-O bond of hydrogen peroxide more efficiently than water [34] resulting in higher turnovers and yields. It may also assist in the formation of a peracid that coordinates to the metal and is cleaved to form a metal-based oxidant [35].

When MeCN:CH_2Cl_2 was used as solvent system, the selectivity towards alcohol increases significantly, but with low overall oxidative activity (Table 1, entry 3). A higher loading of terminal oxidant decreases the A/K ratio (Table 1, entry 4), consistent with earlier reports on related systems by Reedijk *et al.* [36] In the oxidation of cyclohexane using $[Fe(pca)_2(py)_2]$py (pca$^-$ = pyrazine-2-carboxylate; py = pyridine) as catalyst and H_2O_2 as oxidant, these investigators found a decrease in product yield and the A/K ratio (from 2.4 to 2) on increasing the number of equivalents of H_2O_2 from 10 eq. to 100 eq. In order to investigate the potential role of oxygen as a key reactant in formation of the active catalytic species, the reaction was performed under inert atmosphere (Argon) using H_2O_2 as the sacrificial oxidant (Table 1, entry 5). The conversion was slightly lower than the corresponding reaction run under air/H_2O_2 (entry 2), indicating that O_2 does not play a significant role in the oxidation mechanism.

Table 1
Additive effects on cyclohexane oxidation using **1** as catalyst precursor.[a]

Entry	Additive	Conversion[%]	A/K ratio
1	—	79	0.6
2[b]	Acetic acid	98	0.7
3[c]	CH_2Cl_2	10	5
4[d]	5xH_2O_2	89	0.2
5[e]	Ar	93	0.6

[a] [Complex **1**] 1.8×10^{-4} M; alkane, 1.0 mM; H_2O_2 2.5 mM (33% *v*/v H_2O_2 in water), MeCN as solvent (1.5 ml). The results were analyzed *via* GC–MS using 1,2-dichlorbenzene as internal standard.
[b] 1.5 ml solvent (MeCN:Acetic acid 1.0:0.5 ml), reaction occurred in open air.
[c] 1.5 ml solvent (MeCN:CH_2Cl_2 1.0:0.5).
[d] 5 equiv. H_2O_2 is used instead of 2.5 equiv.
[e] 1.0 mM substrate; H_2O_2 2.5 mM (33% v/v H_2O_2 in water), MeCN: Acetic acid 1.0:0.5 ml as solvent and under Ar atmosphere.

Next, we studied the catalytic reactivity of complex **1** using a series of substrates. Oxidation of methylene sites in simple cycloalkanes (Table 2, entries 1–3) was accomplished, affording the corresponding products in 90–98% yields with an almost 1:1 A/K ratio. Interestingly, the more challenging linear alkanes, such as *n*-octane and *n*-decane, were preferentially oxidized at C_2 in 32–52% combined yields.

Cis and *trans*-1,2-dimethylcyclohexane are often used as diagnostic substrates to probe the lifetime of any emerging alkyl radical in alkane hydroxylation reactions. High retention of the original configuration is consistent with metal-based oxidation or evidence for the formation of very short lived alkyl radicals [21b,29,37]. With **1**/H_2O_2, *cis*-1,2-dimethylcyclohexane is preferentially oxidized at the tertiary site in 42% yield while for *trans*-1,2-dimethycyclohexane, possessing sterically more protected tertiary C-H bonds, oxidation occurs with high preference towards the methylene sites (Table 2, entries 7 and 8). The enantiomeric excesses may be anticipated from consideration of the bond dissociation energies (BDEs); the C-H bonds on the tertiary carbons should and often do react more quickly [38]. Upon reaction with the *trans*- isomer, activation of the C-H bonds on secondary carbons is favored, albeit only slightly. Isopropyl-cylohexane is also oxidized in the tertiary position only, with 4% yield (Table 2, entry 9).

As shown with a series of alkene substrates, the catalyst is capable of oxidizing alkenes with good conversions and turnover numbers (TONs) (Table 2, entries 10–13). Epoxide products from aliphatic alkene substrates suggest a mechanism involving a two electron oxidant [39]. Similar product distributions have been reported by Feng et al., using a Pd(II) complex of a dipyridyl based ligand [40].

Interestingly, the styrene oxidation gives benzaldehyde with an excellent yield and selectivity (Table 2, entry 11, 93% and 90% respectively). This points towards the possible formation of a carbon radical intermediate, which may readily react with dioxygen to form benzaldehyde [41]. Hu *et al.* have observed selective formation of benzaldehyde from styrene with Schiff base-modified ordered mesoporous silica materials impregnated with transition metal-monosubstituted Keggin-type polyoxometalates [42]. They proposed that these results indicate the presence of transient high-valent metal-oxido species that are formed via metal-peroxido intermediates and react with the styrene substrate to form benzaldehyde as a major product together with a trace amount of styrene oxide.

Examination of the product distributions and yields (conversions) for different substrates provides further indications that the oxidations proceed by formation of metal-oxido intermediates, but also significant involvement of radical intermediates in some cases. The small cyclic alkanes cyclohexane and cyclopentane (entries 1 and 2, Table 2) give the best turnover numbers and turnover frequencies by a considerable margin. It appears that both the radical and metal oxido pathways are effective in oxidation of these substrates, whereas for a corresponding alkene (*e.g.* cyclohexene, entry 10), it is mainly the oxidation pathway involving a metal-oxido intermediate that is effective, proceeding via an epoxide intermediate and resulting in formation of diols and corresponding ketones [43]. The fact that the radical pathway plays such a significant role in the case of the small cyclic alkanes leads to significantly higher conversions than for the alkenes.

Steric factors may also influence the outcome of a metal-based oxidation pathway. Inclusion of methyl units on substrate backbones induces steric hindrance, hence lowering the reactivity further. It may be noted that cyclohexane and cyclopentane are the least sterically bulky substrates that have been tried, and that we can expect steric discrimination for approach of the substrates to the iron complex, with

Table 2
Catalytic oxidation reactions using **1** as catalyst precursor.

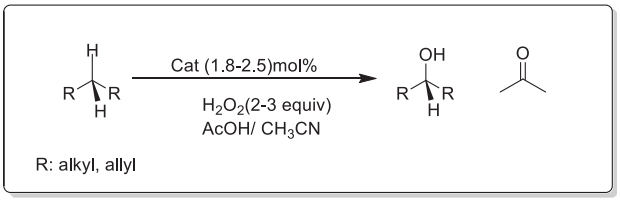

Entry	Substrate	Time	Products (Yield[%])[c]	TON
1		3	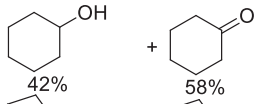 42% + 58%	100
2		3	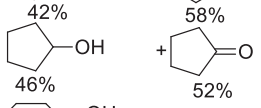 46% + 52%	100
3		8	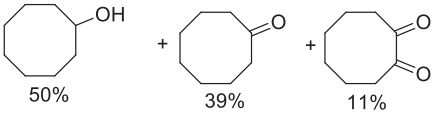 50% + 39% + 11%	69
4	*n*-C_8H_{18}	16	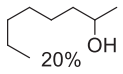 20% + 3-ol 9% + 2-one 9% + 3-one 5% + 4-one 8%	27
5	*n*-$C_{10}H_{20}$	16	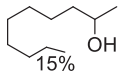 15% + 3-ol 2% + 2-one 5% + 3-one 4% + 4-one 6%	15
6		16	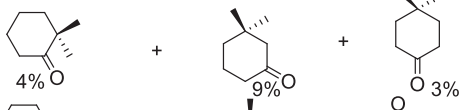 4% + 9% + 3%	8
7		16	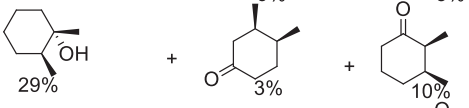 29% + 3% + 10%	22
8		16	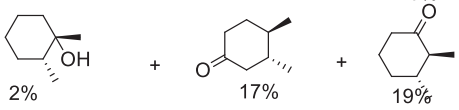 2% + 17% + 19%	20
9	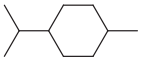	16	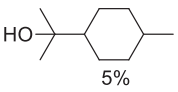 5%	3
10[b]		3	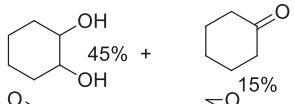 45% + 15%	20
11[b]	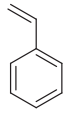	2	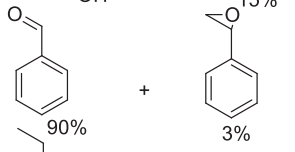 90% + 3%	30
12[b]	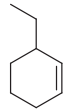	3	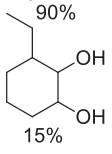 15%	15
13[c]	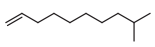	16	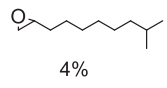 4%	4

[a] Reaction conditions: catalyst **1**: substrate: oxidant ratios are 1.8:100:250, MeCN:acetic acid (1.0:0.5 ml) as solvent, 45 °C. The products were analyzed by GC–MS using 1,2-dichlorobenzene as an internal standard. Each experiment was repeated 3 times and the values above are the averages of the runs. [b.] reaction time 2–3 h. [c.] No other product is formed.

the uncoordinated pendant arm of the ligand adding increased steric hindrance and emulating a second coordination sphere.

In order to enable a comparison of the present oxidation system to related systems, the oxidation of the benchmark substrate cyclohexane by a number of diiron(III) complexes with different terminal oxidants is listed in Table 3. It may be noted that the alcohol/ketone ratios are low (on the order of 0.5–1.5, entries 1–3 and 10–12) when hydrogen peroxide is used as an oxidant, but considerably higher (on the order of 6 or higher, entries 4–9) when the strong oxygen donor *m*-CPBA is used. The latter oxidant is known to be able to generate high-valent metal-oxido complexes and thus supports a metal-based oxidation pathway. Of the hydrogen peroxide-based systems that are compared, the present system, which incorporates acetic acid as an additive, gives the best substrate conversions and yields Table 4.

2.5. Detection of intermediates in oxidation reactions

Low temperature UV–Vis spectroscopy has been extensively used to study the relatively unstable iron-peroxido and iron-oxido intermediates that are involved in oxidative C-H bond activation catalyzed by non-heme iron complexes [46,47].

Several other reactive intermediates are possible when a non-heme iron complex is activated with an H_2O_2 /acetic acid mixture. Based on DFT studies, Wang *et al*. have proposed the formation of ferric peracetate and an oxo-ferryl-AcO$^{\bullet}$ radical from $[Fe(S,S\text{-PDP})(NCMe)_2]^{2+}$ (White's catalyst, PDP = 2-[[2-(1-(pyridin-2-ylmethyl)pyrrolidin-2-yl)pyrrolidin-1-yl]methyl]pyridine) [48]. Previously, using low-temperature UV–Vis spectroscopy and ESI-MS at rapid positive detection mode, we could propose formation of a high valent diiron(IV) oxido-peroxido $[Fe(IV)_2(\mu\text{-}O)(\mu\text{-}O_2)(LiDPCPMPP)_2]^{2+}$ species during C-H bond activation when a 1:1 combination CH_3COOH and H_2O_2 was used as oxidant and $[Fe_2(\mu\text{-}O)(LiDPCPMPP)_2](ClO_4)_2$ as catalyst [13c].

In an initial attempt to monitor the reaction of **1** with H_2O_2 at room temperature, the absorptions at 334 and 289 nm (Fig. 5(a)) were found to disappear immediately upon addition of H_2O_2. This indicates decomposition of **1**, which may be caused by the instability of iron in higher oxidation states at room temperature (Fig. S1). Further spectroscopic studies were therefore carried out at low temperature. The reaction of **1** with CH_3COOH and H_2O_2 (1:1, prepared from a 50% H_2O_2 solution) was studied at 228 K in a solvent mixture of acetonitrile and dichloromethane (1:1 *v*/v); the solvent:CH_3COOH:H_2O_2 ratio was 3:1:1. Upon addition of CH_3COOH, the reddish brown color (λ_{max} = 289, 334, 498 nm) of **1** in acetonitrile/CH_2Cl_2 solution immediately turned blue (λ_{max} = 289, 334, 538 nm, Fig. 5(a)), and in a few minutes after the addition of H_2O_2 at 228 K, the color turned greenish-blue (a broad band at 590 nm, *cf*. Fig. 5(b)). The greenish-blue color was stable at 228 K for 5 h.

Low temperature time-resolved UV–Vis spectroscopic measurements were performed by the direct addition of H_2O_2 + acetic acid (1:1) to a dichloromethane solution of **1** at 228 K, leading to the above-mentioned color changes from purple to blue-green. However, no isosbestic points could be detected, suggesting the existence of additional chemical steps [49]. Slow warming of the blue-green solution to room temperature led to a color change to pale yellow and concomitant evolution of oxygen gas as confirmed by the pyrogallate test (a colorless ethanol solution of potassium pyrrogalate $[C_6H_3(OK)_3]$ turns brownish-purple [3-hydroxy-1,3-benzenequinone] immediately on exposure to the gas). The evolution of oxygen is evidently a part of a decomposition process of unknown nature.

We posit that the blue color arises from a dinuclear iron-peroxido species. Earlier studies on μ-1,2-O_2^{2-} diiron(III) complexes, where the two metal ions are bridged by a carboxylate, as well as a dinucleating ligand incorporating a bridging alkoxide, have reported similar absorption spectra and a blue-green color [48,50]. The broad nature of the 590 nm band may be attributed to the overlap of the peroxido band with the phenoxide to Fe(III) charge transfer band. The decrease in absorbance at 590 nm with an increase in temperature is consistent with the expected instability of a putative peroxido species [51]. Unfortunately, the highly fluorescent nature of the complex prevented us from obtaining meaningful Raman spectra that might corroborate the existence of a peroxido-bridged dinuclear species.

The observed product distribution for the catalytic oxidation of styrene (*vide supra*), demonstrating a high selectivity towards benzaldehyde, and the retention of stereostructures of *cis*- and *trans*-1,2 dimethyl cyclohexane in the oxidation, are consistent with a metal-based oxidation mechanism, involving a high valent metal-oxido complex [39a,46b,52]. On the other hand, the alcohol:ketone ratios are, in general, low and solvent-dependent. These low A/K ratios suggest that radical-based, Fenton-like, oxidation reactions also take place.

3. Summary and conclusions

In this work, we describe a dinuclear iron complex that functions as a (pre)catalyst for oxidation of alkanes and alkenes with good stereoselectivity. The new pro-ligand HDPEAMP and the complex $[Fe_2(\mu\text{-}O)(\mu\text{-}OAc)(DPEAMP)_2](OCH_3)$ (**1**) have been prepared and fully characterized. A detailed study on the oxidative catalytic activity of complex **1** has been performed, using several hydrocarbons as substrates. In an attempt to understand the nature of the active catalyst, low-temperature UV–Vis spectroscopic studies have been performed. We propose that a key step in the catalytic reaction is the formation of a ferric dinuclear peroxido-bridged species of unknown structure, resembling the initial

Table 3
Ligands used (Fig. 4) to prepare diiron complexes, corresponding cyclohexane oxidation products, TON and oxidant used.

Entry	*Ligand used*	*Cyclohexane oxidation Products (yields)*	*TON*	*Oxidant*	*Ref*
1	**DPEAMP**	Cyclohexanol (42%), Cyclohexanone (58%)[a]	100	H_2O_2/AcOH	*this work*
2	**DPCPMPP**	Cyclohexanol (18%), Cyclohexanone (15%)[b]	51	H_2O_2/AcOH	[13b]
3	**IPCPMP**	Cyclohexanol (11%), Cyclohexanone (9%)[c]	19	H_2O_2	[13a]
4	**L1 (TPA)**	Cyclohexanol (84%), Cyclohexanone (13%)[d]	431	*m*-CPBA	[44]
5	**L2**	Cyclohexanol (87%), Cyclohexanone (10%)[d]	494	*m*-CPBA	[44]
6	**L3**	Cyclohexanol (86%), Cyclohexanone (11%)[d]	456	*m*-CPBA	[44]
7	**L4**	Cyclohexanol (87%), Cyclohexanone (10%)[d]	513	*m*-CPBA	[44]
8	**L5**	Cyclohexanol (82%), Cyclohexanone (13%)[d]	451	*m*-CPBA	[44]
9	**L6**	Cyclohexanol (85%), Cyclohexanone (11%)[d]	390	*m*-CPBA	[44]
10	**L7**	Cyclohexanol (4%), Cyclohexanone (4.8%)[e]	0.5	H_2O_2	[45]
11	**L8**	Cyclohexanol (4.6%), Cyclohexanone (5.8%)[e]	0.3	H_2O_2	[45]
12	**L9**	Cyclohexanol (4.5%), Cyclohexanone (7.1%)[e]	0.1	H_2O_2	[45]

[a] *Catalyst (0.2 mM), Substrate (1 mM), H_2O_2(2.5 mM, 33% v/v H_2O_2in water), in MeCN:CH_3COOH (2:1) at 45 °C.*
[b] *Catalyst (0.02 mmol), Substrate (2 mmol), H_2O_2(10 mmol) in MeCN:CH_3COOH (100:3) at 30 °C.*
[c] *Catalyst = 0.7 mM and Catalyst : H_2O_2: Substrate = 1 : 140 : 1000 at room temperature.*
[d] *Catalyst (1 × 10^{-3}mM), Substrates (3 M), m-CPBA (0.8 M) in CH_2Cl_2: MeCN mixture (4:1) at room temperature.*
[e] *Catalyst:H_2O_2: Substrates (1:100:1000) in MeCN at room temperature.*

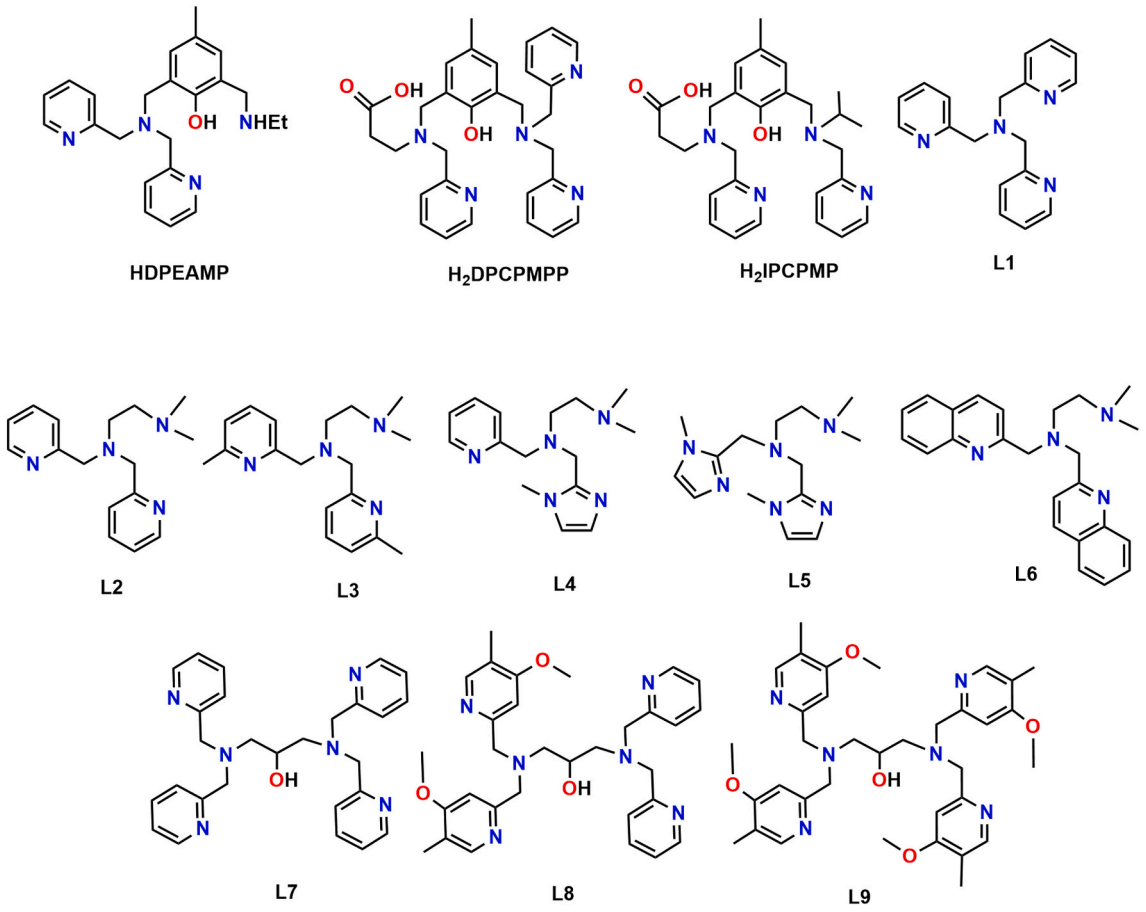

Fig. 4. Depiction of ligands used to prepare diiron complexes for cyclohexane oxidation (*cf.* Table 3).

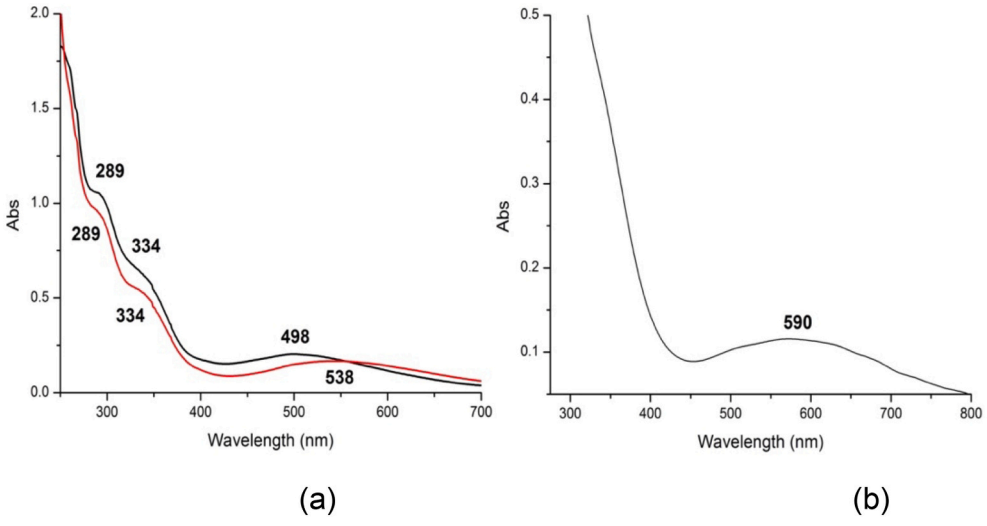

Fig. 5. UV–Vis spectroscopic study of complex **1** a) in acetonitrile(black), acetonitrile + acetic acid (3:1)(red) b) acetonitrile + dichloromethane + acetic acid + H_2O_2 (1.5:1.5:1:1) at 228 K.

formation of intermediate P in the catalytic cycle of soluble methane mono-oxygenase.

The nature of the oxidative products, the stereoselectivity in the catalytic oxidation of 1,2-dimethylcyclohexane, and the formation of benzaldehyde (90%) and styrene oxide (3%) as the oxidation products from styrene, indicate a non-radical mechanism that possibly involves a high-valent iron oxido complex as a transient intermediate and active oxidant. However, the alcohol:ketone ratios in the oxidation reactions suggest that such metal-based oxidation occurs in parallel with radical-based mechanisms. These observations are consistent with our previous studies on oxidation reactions effected by complexes containing the Fe (III)-O-Fe(III) motif [13].

4. Experimental section

4.1. Materials and methods

The starting material 2-hydroxy-3-(hydroxymethyl)-5-methylbenzaldehyde (**a**, *cf*. Scheme 1) was prepared from the selective oxidation of (2-hydroxy-5-methyl-1,3-phenylene)dimethanol using 6 eq. of MnO_2, following a published procedure [53]. All other chemicals and solvents were of analytical or spectroscopic grade purchased from Sigma Aldrich, Fischer chemicals or VWR, and were used without further purification. The ^{1}H NMR spectra were recorded on a Varian Unity 500 MHz spectrometer. Infrared spectra were recorded on KBr pellets in the 4000–400 cm^{-1} range on a Nicolet Avatar 360 FTIR spectrometer. Mass spectrometry was performed with a Bruker HCT Ultra mass spectrometer in the ESI mode. UV–Vis spectra were recorded on a Cary 300 UV–Vis spectrometer. The low-temperature UV–Vis spectra were measured with a quartz transmission probe (1 mm, Hellma Analytics). Mössbauer spectra were recorded at 80 K with a ^{57}Co source in a Rh matrix, using an alternating constant-acceleration Wissel Mössbauer spectrometer operated in the transmission mode and equipped with a Janis closed-cycle helium cryostat or with a Mössbauer-Spectromag cryostat.

Analytical achiral GC was performed on an Agilent 6850 GC with FID detector using an Agilent DB-WAX (30.0 m × 0.25 mm) column with He carrier gas flow. Chiral GC was performed on an Agilent 6850 GC with FID detector. The ^{1}H NMR spectra of the analytes were recorded on a Varian Gemini 200 apparatus or a Varian Mercury 300 MHz spectrometer. All secondary alcohols gave spectroscopic data in agreement with those reported in the literature. GC–MS measurements were performed using 1,2-dichlorobenzene as internal standard and the products were compared to authentic purchased ones.

4.2. Synthetic procedures

4.2.1. Synthesis of 2-((bis(pyridin-2-ylmethyl)amino)methyl)-6-(hydroxymethyl)-4-methylphenol (b)

Bis(pyridin-2-ylmethyl)amine (1.2 g, 6.022 mmol) was dissolved in dichloromethane (15 ml) and 4 Å molecular sieves were added. A total of 25 ml of a dichloromethane solution of **a** (1 g, 6.0 mmol, Scheme 2) was added dropwise to this solution under continuous stirring at room temperature. The color of the mixture turned from yellow to orange. After 2 h, $NaBH(OAc)_3$ (2.3 g, 10.85 mmol) was added at room temperature and was stirred for 12 h. Afterwards a saturated $NaHCO_3$-solution (15 mL) was added and the mixture was stirred for 1 h. The resulting mixture was filtered and extracted with dichloromethane (3 × 20 mL). The organic layers were combined, dried over Na_2SO_4, filtered and concentrated under vacuum. A total of 1.76 g (yield 84%) of **b** was obtained as a yellow-brown solid. ^{1}H NMR (500 MHz) $CDCl_3$: δ 8.45 (m, 2H), 7.50 (m, 2H), 7.21 (m, 2H), 7.04 (m, 2H), 6.89 (s, 1H), 6.71 (s, 1H), 4.65(s, 2H), 3.76(s, 4H), 3.65(s, 2H), 2.13(s, 3H).

4.2.2. Synthesis of 2-((bis(pyridin-2-ylmethyl)amino)methyl)-6-((ethylamino)methyl)-4-methyl-phenol (HDPEAMP)

A total of 1 g (2.86 mmol) 2-((bis(pyridin-2-ylmethyl)amino) methyl)-6-(hydroxymethyl)-4-methylphenol (**b**) was dissolved in 5 ml of dichloromethane and 12 ml of $SOCl_2$ was added dropwise to the solution with continuous stirring. The yellow color changed to green immediately upon addition of thionyl chloride and became brown after ca 30 min. The mixture was stirred at room temperature for 12 h and dried under high vacuum overnight to remove excess HCl and $SOCl_2$, giving 1.02 g (2.78 mmol) of 2-((bis(pyridin-2-ylmethyl)amino)methyl)-6-(chloromethyl)-4-methylphenol (**c**) as a pale brown solid. This solid (**c**) was dissolved in EtOH and cooled to −40 °C. Triethylamine was added dropwise until white fumes of $Et_3NH^+Cl^-$ ceased to form, after which the solution was allowed to warm to room temperature and an excess of $EtNH_2$ (0.8 ml, 14.38 mmol) was added to the stirring solution, which was subsequently refluxed for 3 h, during which the reaction was monitored by thin layer chromatography (every 20 min) to detect completion of the reaction. After 3 h, the solvent was removed using a rotary evaporator. A total of 20 ml of water was added and the product was extracted with dichloromethane (3 × 20 ml). The organic layers were combined and dried over anhydrous Na_2SO_4, which resulted in the formation of a yellowish hygroscopic solid. A total of 0.657 g (1.74 mmol, yield 61%) of pale yellow solid of HDPEAMP was obtained after drying overnight under vacuum. Being quite hygroscopic in nature, special care was taken to keep the yellow solid (HDPEAMP) dry by keeping it in a vacuum desiccator for two days. ^{1}H (500 MHz) CD_3OD: δ 8.4 (m, 2H), 7.47 (m, 2H), 7.12 (s, 2H), 6.99 (m, 2H), 6.84 (m, 1H), 3.67 (s, 4H), 3.53 (s, 4H), 2.85 (q, 2H), 2.05 (s, 3H), 1.01 (t, 3H). IR (KBr, cm^{-1}): 3432(b, s), 3051(w), 2976(s), 2939(s), 2738(w), 2677(s), 2492 (s), 2022(b, s), 1596(s), 1570(s), 1473(s), 1397(s), 1215(s), 1125(s), 1037(s), 958(s), 792(s), 766(s), 634(s). ^{13}C NMR (500 MHz, CD_3OD): δ = 157.92, 148.27, 137.38, 132.14, 130.99, 130.43, 129.88, 128.17, 127.55, 123.55, 122.59, 62.47, 58.61, 55.61, 52.39, 34.76, 19.29, 11.77.ESI-MS calculated for $C_{23}H_{29}N_4O$ ($M\text{-}H^+$): 377.2; found 377.1.

4.2.3. Synthesis of $[Fe_2(\mu\text{-}O)(\mu\text{-}OAc)(DPEAMP)_2](OCH_3)$ (1)

Caution:*Transition metal perchlorates should be handled with great care and be prepared in small quantities, as metal perchlorates are hazardous and may explode upon heating.*

To a methanol solution of 0.5 g (1.32 mmol) of HDPEAMP, 0.231 g of $Fe(OAc)_2$ (1.32 mmol) was added and the solution was stirred for 2 h at room temperature. The yellow color of the ligand solution turned dark green immediately after addition of iron(II) acetate, and changed further to dark brown after approximately half an hour. A total of 0.324 g of Na (ClO_4) (2.65 mmol) was added and the resultant solution was stirred for an additional hour. No appreciable color change was visible upon the addition of Na(ClO_4). The solution was filtered through a celite pad to remove iron hydroxide impurities. The filtrate was taken in a 50 ml round bottom flask and the solvent was removed using a rotary evaporator. Fifteen ml of ice cold water was added to remove unreacted perchlorate salt. After decanting the water, the flask was kept under high vacuum overnight, which gave 0.784 g (62.97%) of [Fe_2(μ-O)(μ-OAc)(DPEAMP)$_2$](OCH_3) as a dark brown powder. This powder was redissolved in dry MeOH and slow vapor diffusion of diethyl ether into the methanol solution gave rise to dark brown crystals suitable for X-ray diffraction. Because of the hygroscopic nature of the crystals, they were stored under vacuum.

UV–Vis (CH_3CN): λ_{max} = 498 nm (ε = 1200 M^{-1} cm^{-1}), 334 nm (ε = 3400 M^{-1} cm^{-1}) and 289 nm (ε = 5800 M^{-1} cm^{-1}). ^{57}Fe Mössbauer (80 K) δ = 0.49 mm/s; ΔE_Q = 1.38 mm/s; ESI-MS in acetonitrile solution, calculated for $C_{23}H_{27}N_4OFe^+$ (mononuclear species – Fe(DPEAMP)): 431.15; found 429.9.

Anal. Calcd for $C_{49}H_{77}Cl_3Fe_2N_8O_{25}$ [Fe_2(μ-O)(μ-OAc)(DPEAMP)$_2$](OCH_3).3$HClO_4$.7H_2O]: C, 42.15; H, 5.56; N, 8.03. Found: C, 42.16; H, 5.69; N, 7.73. IR (KBr, cm^{-1}): 3440(b, s), 2958(b), 2917(b), 2855(b), 1605(s), 1478(s), 1262(s), 1151(s), 1115(s), 1086(s), 1025(s), 849(s) 559(s).

4.3. X-Ray crystallography

Dark brown single crystals of [Fe_2O(OAc)(DPEAMP)$_2$](OCH_3) of reasonable X-ray quality were grown by slow vapor diffusion of diethyl ether into a concentrated methanolic solution of the iron complex. X-ray data were collected on a STOE IPDS II diffractometer with an area detector (graphite monochromated Mo-Kα radiation, λ = 0.71073 Å) by use of ω scans at 133 K. Data reduction was performed using STOE X-Red and was corrected for absorption and decay by X-shape [54]. The structure was solved by charge flipping as implemented in Super flip [55] and refined against F^2 in JANA2006 [56]. The metal atom positions and most of the ligand positions were quickly identified, but the parts of the ligands relatively far away from the metal centers showed large thermal displacement parameters. The methyl residue of the bridging

acetate is disordered by symmetry since it occupies a position on a two-fold axis, forcing rotational disorder of the hydrogen positions. Further, as the terminal ethyl group(s) bound to N4 is pointing away from the metal center and into the surrounding solvent shell, this group shows very high thermal displacement parameters and is most probably conformationally disordered. Finally, it was not possible to locate all solvent molecules, and some of these that were found also show large thermal motion and/or partial occupancy as might be expected in a structure with such a large solvent content. Final agreement parameters converged to $R_1 = 0.086$ and $R_w(F^2) = 0.170$, showing that substantial electron density is unaccounted for in the final model, but this residual density is located in the solvent subspace or on the disordered residues while the metal centers and the parts of the ligands directly neighboring these are very well ordered.

4.4. General oxidation procedures

Conversion of cyclooctane (as an example)**:** Cyclooctane (114 mg, 134 ml, 1 mmol) was added to a solution of **1** (0.01 mmol) in MeCN: acetic acid (1.5:0.5 ml). After the addition of H_2O_2 (33% in H_2O; 227 μL, 2.5 mmol), the reaction mixture was stirred vigorously at 45 °C for 3 h. The mixture was then allowed to cool to room temperature. The organic phase was extracted with Et_2O (3 × 1 ml), washed with brine and dried ($MgSO_4$). After filtration, the solvents of the filtrate were evaporated (rotary evaporator). The remaining mixture was separated by column chromatography (silica gel; diethyl ether: pentane = 1:20 as eluent) and the product was analyzed by GC–MS using 1,2-dichlorobenzene as an internal standard.

4.5. GC analysis

In the oxidation of *cis*-1,2-dimethylcyclohexane the reaction mixture was directly passed through a short path of silica to remove the iron catalyst followed by elution with ethyl acetate (2 mL). Calibration curves were obtained from commercial products purchased from Aldrich or TCI, when available, or from pure isolated products obtained from a catalytic reaction. The concentrations of each organic product were calibrated relative to that of an internal standard (dichlorobenzene) with a known concentration. Substrate conversions and product yields were calculated relative to the internal standard integration. The product yields should not be confused with product distribution ratios. All experiments were repeated at least three times, and the reported values are the average of all experiments.

CRediT authorship contribution statement

Biswanath Das: Conceptualization, Investigation, Writing – original draft, Writing – review & editing. **Afnan Al-Hunaiti:** Investigation, Methodology, Writing – original draft, Writing – review & editing. **Akina Carey:** Investigation. **Sven Lidin:** Investigation, Validation, Writing – review & editing. **Serhiy Demeshko:** Investigation, Validation, Writing – review & editing. **Timo Repo:** Supervision, Project administration, Funding acquisition, Writing – review & editing. **Ebbe Nordlander:** Conceptualization, Supervision, Project administration, Funding acquisition, Writing – review & editing.

Declaration of Competing Interest

The authors declare that there are no conflicts of interest related to the present manuscript.

Acknowledgements

This paper is dedicated to the memory of Professor Richard H. Holm, a pioneer in bioinorganic chemistry, an outstanding scientist who adhered to the highest standards, and a good mentor. The research has been carried out within the framework of the International Research Training Group *Metal Sites in Biomolecules: Structures, Regulation and Mechanisms*, and has been supported by COST ActionCM1003. We thank the European Union for an Erasmus Mundus fellowship to B·D., Dr. Ivan Castillo Pérez and Prof. Franc Meyer for useful discussions, and Sven Neudeck for help with mass spectrometric measurements. A.A-H. is grateful for the financial support from the Inorganic Materials Chemistry Graduate Program and Tekes - the Finnish Funding Agency for Technology and Innovation (project 40099/10).

Appendix B. Supplementary data

UV–Vis spectra of complex **1** in different solvent mixtures and pH, cyclic voltammogram of **1**, Mössbauer spectrum of **1**. CCDC 2131633 contains the supplementary crystallographic data for this paper. This data can be obtained free of charge from The Cambridge Crystallographic Data Centre via www.ccdc.cam.ac.uk/data_request/cif. Supplementary data to this article can be found online at [https://doi.org/10.1016/j.jinorgbio.2022.111769].

References

[1] (a) D. Webb, T.F. Jamison, Chem. Sci. 1 (2010) 675–680;
(b) A.E. Shilov, G.B. Shul'pin, Chem. Rev. 97 (1997) 2879–2932.
[2] M.O. Ross, A.C. Rosenzweig, J. Biol. Inorg. Chem. 22 (2017) 307–319.
[3] (a) J. Colby, H. Dalton, Biochem. J. 171 (1978) 461–468;
(b) A.C. Rosenzweig, P. Nordlund, P.M. Takahara, C.A. Frederick, S.J. Lippard, Chem. Biol. 2 (1995) 409–418;
(c) A.C. Rosenzweig, C.A. Frederick, S.J. Lippard, P. Nordlund, Nature 6 (1993) 537–543;
(d) R. Banerjee, J.C. Jones, J.D. Lipscomb, Annu. Rev. Biochem. 88 (2019) 409–431;
(e) R. Banerjee, Y. Proshlyakov, J.D. Lipscomb, D.A. Proshlyakov, Nature 518 (2015) 431–434.
[4] (a) M.A. Culpepper, A.C. Rosenzweig, Crit. Rev. Biochem. Mol. Biol. 47 (2012) 483–492;
(b) M.O. Ross, A.C. Rosenzweig, J. Biol. Inorg. Chem. 22 (2017) 307–319.
[5] S.M. Smith, S. Rawat, J. Telser, B.M. Hoffman, T.L. Stemmler, A.C. Rosenzweig, Biochemistry 50 (2011) 10231–10240.
[6] (a) A.J. Jasniewski, L. Que Jr., Chem. Rev. 118 (2018) 2554–2592;
(b) A.A. Shteinman, M. Mitra, Inorg. Chim. Acta 523 (2021), 120388;
(c) A.A. Shteinman, Kin. Catal. 61 (2020) 339–359.
[7] (a) L. Shu, J.C. Nesheim, K. Kauffmann, E. Munck, J.D. Lipscomb, L. Que Jr., Science 275 (1997) 515–518;
(b) E.C. Wilkinson, Y. Dong, Y. Zang, H. Fujii, R. Fraczkiewicz, G. Fraczkiewicz, R. S. Czernuszewicz, L. Que Jr., J. Am. Chem. Soc. 120 (1998) 955–962;
(c) H. Basch, K. Mogi, D.G. Musaev, K. Morokuma, J. Am. Chem. Soc. 121 (1999) 7249–7256.
[8] (a) G. Xue, R.D. Hont, E. Münck, L. Que Jr., Nat. Chem. 2 (2010) 400–405;
(b) A.A. Shteinman, FEBS Lett. 362 (1995) 5–9.
[9] (a) M.S. Chen, M.C. White, Science 318 (2007) 783–787;
(b) P.E. Gormisky, M.C. White, J. Am. Chem. Soc. 135 (2013) 14052–14055;
(c) T.J. Osberger, D.C. Rogness, J.T. Kohrt, A.F. Stepan, Nature 537 (2016) 214–219;
(d) (13988–1409) M.C. White, J. Zhao, J. Am. Chem. Soc. 140 (2018).
[10] J. England, G.J.P. Britovsek, N. Rabadia, A.J.P. White, Inorg. Chem. 46 (2007) 3752–3767.
[11] G.J.P. Britovsek, J. England, A.J.P. White, Inorg. Chem. 44 (2005) 8125–8134.
[12] (a) S. Banerjee, A. Draksharapu, P.M. Crossland, R. Fan, Y. Guo, M. Swart, L. Que Jr., J. Am. Chem. Soc. 142 (2022) 4285–4297;
(b) G.T. Rohde, G. Xue, L. Que, Faraday Discuss. (2021) (DOI:10.1039./D1FD00066G).
[13] (a) M. Jarenmark, E.A. Turitsyna, M. Haukka, A.A. Shteinman, E. Nordlander, New J. Chem. 34 (2010) 2118–2121;
(b) B. Das, A. Al-Hunaiti, M. Haukka, S. Demeshko, S. Meyer, A.A. Shteinman, F. Meyer, T. Repo, E. Nordlander, Eur. J. Inorg. Chem. (2015) 3590–3601;
(c) B. Das, A. Al-Hunaiti, B.N. Sanchez-Eguia, E. Zeglio, S. Demeshko, S. Dechert, S. Braunger, M. Haukka, T. Repo, I. Castillo, E. Nordlander, Front. Chem. 7 (97) (2019) 1–12.
[14] D.M. Kurtz Jr., Chem. Rev. 90 (1990) 585–606.
[15] R.E. Norman, S. Yan, L. Que, J.G. Backes, J. Ling, J. Sanders-Loehr, J.H. Zhang, C. J. O'Connor, J. Am. Chem. Soc. 112 (1990) 1554–1562.
[16] R.C. Reem, J.M. McCormick, D.E. Richardson, F.J. Devlin, P.J. Stephens, R. L. Musselman, E.I. Solomon, J. Am. Chem. Soc. 111 (1989) 4688–4704.
[17] R.N. Mukherjee, T.D.P. Stack, R.H. Holm, J. Am. Chem. Soc. 110 (1988) 1850–1861.
[18] (a) G.B. Deacon, R.J. Phillips, Coord. Chem. Rev. 33 (1980) 227–250;
(b) H. Carlsson, M. Haukka, A. Bousseksou, J.-M. Latour, E. Nordlander, Inorg. Chem. 43 (2004) 8252–8262;

(c) M. Jarenmark, M. Haukka, S. Demeshko, F. Tuczek, L. Zuppiroli, F. Meyer, E. Nordlander, Inorg. Chem. 50 (2011) 3866–3887.
[19] L.H. Do, G. Xue, L. Que, S.J. Lippard, Inorg. Chem. 51 (2012) 2393–2402.
[20] M.H. Sazinsky, J. Bard, A.D. Donato, S.J. Lippard, J. Biol. Chem. 279 (2004) 30600–30610.
[21] (a) J.B.H. Strautmann, C.-G.F. von Richthofen, S. DeBeer, E. George, E. Bill Bothe, T. Glaser, Chem. Commun. (2009) 2637–2639;
(b) J.B.H. Strautmann, S. DeBeer George, E. Bothe, E. Bill, T. Weyhermüller, A. Stammler, H. Bögge, T. Glaser, Inorg. Chem. 47 (2008) 6804–6824;
(c) J.B.H. Strautmann, S. Walleck, H. Bögge, A. Stammler, T. Glaser, Chem. Commun. 47 (2011) 695–697;
(d) T. Glaser, Coord. Chem. Rev. 380 (2019) 353–377.
[22] B. Adam, E. Bill, E. Bothe, B. Goerdt, G. Haselhorst, K. Hildenbrand, A. Sokolowski, S. Steenken, T. Weyhermüller, K. Wieghardt, Chem. Eur. J. 3 (1997) 308–319.
[23] T. Kurahashi, Y. Kobayashi, S. Nagamoto, T. Tosha, T. Kitagawa, H. Fujii, Inorg. Chem. 44 (2005) 5810–5819.
[24] K.L. Stone, A.S. Borovik, Curr. Opin. Chem. Biol. 13 (2009) 114–118.
[25] B-L. Lee, E.A. Karlsson, B. Das, M.D. Kärkäs, T. Åkermark, E.V. Johnston, S. Demeshko, M. Monari, F. Meyer, E. Nordlander, B. Åkermark (unpublished results).
[26] R. Sun, K. Wang, D.-D. Wu, W. Huang, Y.-B. Ou, Acta Cryst E68 (2012), o824.
[27] (a) Q.-R. Cheng, H. Zhou, Z.-Q. Pan, J.-Z. Chen, Polyhedron 30 (2011) 1171–1176;
(b) G. Olivo, O. Cussó, M. Borrell, Miquel Costas, J. Biol. Inorg. Chem. 22 (2017) 425–452.
[28] A. Horn, I. Vencato, A.J. Bortoluzzi, R. Hörner, R.A.N. Silva, B. Spoganicz, V. Drago, H. Terenzi, M.C.B. Oliveira, R. Werner, W. Haase, A. Neves, Inorg. Chim. Acta 358 (2005) 339–351.
[29] M. Costas, K. Chen, L. Que Jr., Coord. Chem. Rev. 200 (2000) 517–544.
[30] X. Wang, S. Wang, L. Li, E.B. Sundberg, G.P. Gacho, Inorg. Chem. 42 (2003) 7799–7808.
[31] T. Nagataki, Y. Tachi, S. Itoh, J. Mol. Catal. A Chem. 225 (2005) 103–109.
[32] T.A. van den Berg, J.W. de Boer, W.R. Browne, G. Roelfes, B.L. Feringa, Chem. Commun. (2004) 2550–2551.
[33] (a) M.C. White, A.G. Doyle, E.N. Jacobsen, J. Am. Chem. Soc. 123 (2001) 7194–7195;
(b) M. Fujita, L. Que Jr., Adv. Synth. Catal. 346 (2004) 190–194;
(c) M.S. Chen, M.C. White, Science 318 (2007) 783–787;
(d) O. Cusso, I. Garcia-Bosch, X. Ribas, J. Lloret-Fillol, M. Costas, J. Am. Chem. Soc. 135 (2013) 14871–14878;
(e) M. Mitra, O. Cusso, S.S. Bhat, M. Sun, M. Cianfanelli, M. Costas, E. Nordlander, Dalton Trans. 48 (2019) 6123–6131.
[34] (a) R. Mas-Ballesté, L. Que Jr., J. Am. Chem. Soc. 129 (2007) 15964–15972;
(b) U.S. Agarwalla, Transit. Met. Chem. 45 (2020) 583–588.
[35] Y. Wang, D. Janardanan, D. Usharani, K. Han, L. Que Jr., S. Shaik, ACS Catal. 3 (2013) 1334–1341.
[36] S. Tanase, P. Marques-Gallego, W.R. Browne, R. Hage, E. Bouwman, B.L. Feringa, J. Reedijk, Dalton Trans. (2008) 2026–2033.
[37] M.S. Chen, M.C. White, Science 327 (2010) 566–571.
[38] (a) C.R. Goldsmith, R.T. Jonas, T.D.P. Stack, J. Am. Chem. Soc. 124 (2002) 83–96;
(b) A. Company, L. Gómez, M. Guell, X. Ribas, J.M. Luis, L. Que Jr., M. Costas, J. Am. Chem. Soc. 129 (2007) 15766–15767;
(c) J. Kaizer, E.J. Klinker, N.Y. Oh, J.-U. Rohde, W.J. Song, A. Stubna, J. Kim, E. Münck, W. Nam, L. Que Jr., J. Am. Chem. Soc. 126 (2004) 472–473;
(d) T. Newhouse, P.S. Baran, Angew. Chem. Int. Ed. 50 (2011) 3362–3374.
[39] (a) L. Vicens, G. Olivo, M. Costas, ACS Catal. 10 (2020) 8611–8631;
(b) J.E.M.N. Klein, D. Mandal, W.-M. Ching, D. Mallick, L. Que Jr., S. Shaik, J. Am. Chem. Soc. 139 (2017) 18705–18713.
[40] B. Feng, Z. Hou, X. Wang, Y. Hu, H. Li, Y. Qiao, Green Chem. 11 (2009) 1446–1452.
[41] J.T. Groves, Z. Gross, M.K. Stern, Inorg. Chem. 33 (1994) 5065–5072.
[42] J. Hu, K. Li, W. Li, F. Ma, Y. Guo, Appl. Catal. A. 364 (2009) 211–220.
[43] A.P.C. Robeiro, E. Spada, R. Bertani, L.M.D.R.S. Martins, Catalysts 10 (2020) 1443.
[44] M. Balamurugan, E. Suresh, M. Palaniandavar, RSC Adv. 11 (2021) 21514–21526.
[45] A. Trehoux, R. Guillot, M. Clemancey, G. Blondin, J.-M. Latour, J.-P. Mahy, F. Avenier, Dalton Trans. 49 (2020) 16657–16661.
[46] (a) M.S. Seo, N.H. Kim, K.-B. Cho, J.E. So, S.K. Park, M. Clemancey, R. Garcia-Serres, J.-M. Latour, S. Shaik, W. Nam, Chem. Sci. 2 (2011) 1039;
(b) J. Chen, Z. Jiang, S. Fukuzumi, W. Nam, B. Wang, Coord. Chem. Rev. 421 (2020) 213443;
(c) S. Fukuzumi, K.-B. Cho, Y.-M. Lee, S. Hong, W. Nam, Chem. Soc. Rev. 49 (2020) 8988–9027.
[47] (a) M.H. Lim, J.-U. Rohde, A. Stubna, M.R. Bukowski, M. Costas, R.Y.N. Ho, E. Münck, W. Nam, L. Que Jr., Proc. Natl. Acad. Sci. U. S. A. 100 (2003) 3665–3670;
(b) S. Meyer, I. Klawitter, S. Demeshko, E. Bill, F. Meyer, Angew. Chem. Int. Ed. 52 (2013) 901–905;
(c) R. R.Mas-Ballesté, L. Que Jr, L. Que Jr., J. Am. Chem. Soc. 129 (2007) 15964–15972.
[48] Y. Wang, D. Janardanan, D. Usharani, K. Han, L. Que Jr., S. Shaik, ACS Catal. 3 (2013) 1334–1341.
[49] F. Avenier, C. Herrero, W. Leibl, A. Desbois, R. Guillot, J.-P. Mahy, A. Aukauloo, Angew. Chem. Int. Ed. 52 (2013) 3634–3637.
[50] (a) Y. Dong, S. Ménage, B.A. Brennan, T.E. Elgren, H.G. Jang, L.L. Pearce, L. Que Jr., J. Am. Chem. Soc. 115 (1993) 1851–1859;
(b) L.H. Do, T. Hayashi, P. Moenne-Loccoz, S.J. Lippard, J. Am. Chem. Soc. 132 (2010) 1273–1275 (For a review of dinuclear Fe(III) μ-peroxido complexes of relevance to sMMO, see reference 6a).
[51] G. Xue, A.T. Fiedler, M. Martinho, E. Münck, L. Que Jr., Proc. Natl. Acad. Sci. U. S. A. 105 (2008) 20615–20620.
[52] (a) C.L. Hill, C.M. Prosser-McCartha, Coord. Chem. Rev. 143 (1995) (1995) 407–455;
(b) M.S. Vad, A. Lennartson, A. Nielsen, J. Harmer, J.E. McGrady, C. Frandsen, S. Mørup, C.J. McKenzie, Chem. Commun. 48 (2012) 10880–10882;
(c) J. Park, Y. Morimoto, Y.-M. Lee, W. Nam, S. Fukuzumi, J. Am. Chem. Soc. 134 (2012) 3903–3911;
(d) S.H. Lee, J.H. Han, H. Kwak, S.J. Lee, E.Y. Lee, H.J. Kim, J.H. Lee, C. Bae, S. N. Lee, Y. Kim, C. Kim, Chem. Eur. J. 13 (2007) 9393–9398;
(e) B.D. Dunietz, M.D. Beachy, Y. Cao, D.A. Whittington, S.J. Lippard, R. A. Friesner, J. Am. Chem. Soc. 122 (2000) 2828–2839.
[53] M. Jarenmark, S. Kappen, M. Haukka, E. Nordlander, Dalton Trans. (2008) 993–996.
[54] (a) X-RED, Version 1.07, STOE & Cie GmbH, Darmstadt, Germany, 1996;
(b) X-SHAPE, Version 1.01, STOE & Cie GmbH, Darmstadt, Germany, 1996.
[55] L. Palatinus, G.J. Chapuis, Appl. Cryst. 40 (2007) 786–790.
[56] V. Petricek, M. Dusek, L. Palatinus, The Crystallographic Computing System, Jana 2006, Institute of Physics, Praha, Czech Republic, 2006.